Fig. 10. RUNX2 suppresses ADR-mediated induction of TAp73. U2OS cells were transfected as described in Fig. 9. Twenty-four hours after transfection, cells were treated with 0.5 µM of ADR or left untreated. Twenty-four hours after treatment, whole cell lysates and total RNA were prepared and analyzed by (A) immunoblotting and (B) RT-PCR, respectively.

described previously [19] using the primary antibodies: mouse monoclonal anti-p53 (DO-1; Santa Cruz Biotechnology, Santa Cruz, CA, USA), mouse monoclonal anti-p73 (Ab-4; NeoMarkers, Fremont, CA, USA), mouse monoclonal anti-γH2AX (2F3; BioLegend, San Diego, CA, USA), rabbit polyclonal anti-p21^{WAF1} (Santa Cruz Biotechnology), rabbit polyclonal anti-phospho-p53 at Ser-15 (Cell Signaling Technology, Beverly, MA, USA), rabbit polyclonal anti-RUNX2 (Cell Signaling Technology), rabbit polyclonal anti-E2F-1 (Cell Signaling Technology), rabbit polyclonal anti-PARP (Cell Signaling Technology), rabbit polyclonal anti-caspase-9 (Cell Signaling Technology) and rabbit polyclonal anti-Actin (20–33; Sigma, St Louis, MO, USA) antibodies. Immunoreactive bands were visualized by an enhanced chemiluminescence system (ECL; GE Healthcare, Little Chalfont, UK) in accordance with the manufacturer's instructions.

Immunoprecipitation

For immunoprecipitation, cells were exposed to 0.5 µM of ADR for 24 h and then lysed in lysis buffer containing 50 mM Tris-HCl (pH 7.5), 150 mM NaCl, 2.7 mM KCl, 1% Triton X-100 and protease inhibitor mixture (Sigma). Equal amounts of cell lysates (500 µg of protein) were first precleared with 30 µL of protein G-Sepharose beads for 1 h at 4 °C and then incubated with monoclonal anti-p73 antibody overnight at 4 °C followed by the incubation with 30 µL of protein G-Sepharose beads for 2 h at 4 °C. The beads were extensively washed with lysis buffer and the immunoprecipitates were eluted by boiling in SDS-sample buffer. The bound proteins were separated by 10% SDS/PAGE.

siRNA interference

Cells were transfected with control siRNA or with siRNA directed against RUNX2 (10 nM) using Lipofectamine 2000 transfection reagent in accordance with the manufacturer's recommendations. Twenty-four hours after transfection, cells were treated with 0.5 µM of ADR or left untreated. Twenty-four hours after treatment, total RNA was prepared and analyzed for the expression level of *RUNX2* by RT-PCR.

Luciferase reporter assay

Cells were seeded at a density of 5 x 10^4 cells per 12-well plate and allowed to attach overnight. Cells were then

RUNX2 — — + +

ADR — + — +
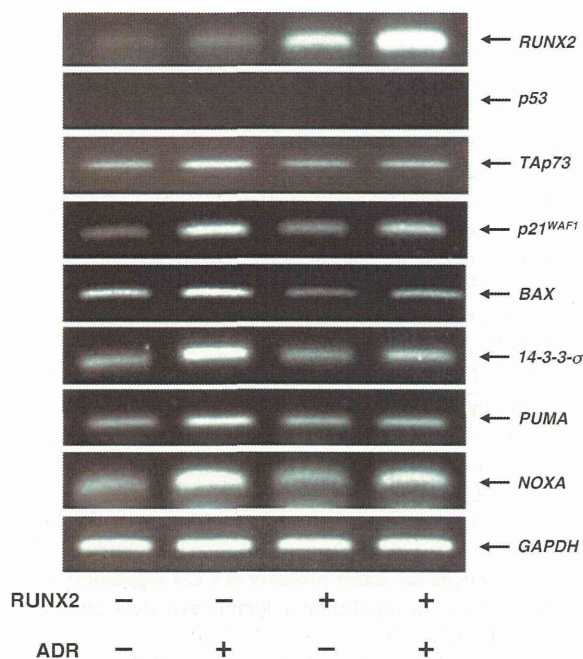
Fig. 11. RUNX2 inhibits ADR-mediated upregulation of *TAp73* in H1299 cells. H1299 cells were transiently transfected with the empty plasmid or with the expression plasmid for RUNX2. Twenty-four hours after transfection, cells were treated with 0.5 µM of ADR or left untreated. Twenty-four hours after treatment, total RNA was prepared and subjected to RT-PCR.

transfected with the constant amount of TAp73α expression plasmid (25 ng), 100 ng of luciferase reporter plasmid carrying p53/p73-responsible human *BAX* or *NOXA* promoter and 10 ng of *renilla* luciferase expression plasmid, together with or without increasing amounts of the expression plasmid for RUNX2. Equal DNA concentration in each experiment (500 ng per well) was maintained by adding the appropriate amounts of the empty plasmid to the DNA mixture. Forty-eight hours after transfection, cell lysates were prepared and their luciferase activities were measured in accordance with the protocol for the dual-luciferase system (Promega, Madison, WI, USA). The resultant firefly luciferase values were normalized by those of *renilla* luciferase. The experiments were performed in parallel and repeated at least three times.

TUNEL assay

TUNEL assay was performed by using an *In Situ* Cell Detection Kit (Roche Applied Science, Mannheim, Germany) in accordance with the manufacturer's protocol. In brief, cells were washed twice in PBS, fixed in freshly prepared 4% paraformaldehyde for 1 h at room temperature, permeabilized with 0.1% Triton X-100 in 0.1% sodium

citrate for 2 min at room temperature, and then incubated with the enzyme solution in a humidified atmosphere for 1 h at 37 °C in the dark. After the reaction, cells were washed in PBS three times and fluorescent images were taken using a confocal microscope.

Statistical analysis

Statistical significance was determined by two-sided paired Student's *t*-test. $P < 0.05$ was considered statistically significant.

Author contributions

TO and HN planned the experiments. TO, HS, MN, KH and HY performed the experiments. TO analyzed the data. MS and KF contributed reagents or other essential materials. TO wrote the paper.

References

1 Prives C & Hall PA (1999) The p53 pathway. *J Pathol* **187**, 112–126.

2 Sionov RV & Haupt Y (1999) The cellular response to p53: the decision between life and death. *Oncogene* **18**, 6145–6157.

3 Vousden KH & Lu X (2002) Live or let die: the cell's response to p53. *Nat Rev Cancer* **2**, 594–604.

4 Vogelstein B & Kinzler KW (1992) p53 function and dysfunction. *Cell* **70**, 523–526.

5 Harris CC (1993) p53: at the crossroads of molecular carcinogenesis and risk assessment. *Science* **262**, 1980–1981.

6 Vogelstein B, Lane D & Levine AJ (2000) Surfing the p53 network. *Nature* **408**, 307–310.

7 Strano S, Dell'Orso S, Mongiovi AM, Monti O, Lapi E, Di Agostino S, Fontemaggi G & Blandino G (2007) Mutant p53 proteins: between loss and gain of function. *Head Neck* **29**, 488–496.

8 Strano S, Dell'Orso S, Di Agostino S, Fontemaggi G, Sacchi A & Blandino G (2007) Mutant p53: an oncogenic transcription factor. *Oncogene* **26**, 2212–2219.

9 Kaghad M, Bonnet H, Yang A, Creancier L, Biscan JC, Valent A, Minty A, Chalon P, Lelias JM, Dumont X *et al.* (1997) Monoallelically expressed gene related to p53 at 1p36, a region frequently deleted in

neuroblastoma and other human cancers. *Cell* **90**, 809–819.

10 Jost CA, Marin MC & Kaelin WG Jr (1997) p73 is a simian p53-related protein that can induce apoptosis. *Nature* **389**, 191–194.

11 Irwin MS, Kondo K, Marin MC, Cheng LS, Hahn WC & Kaelin WG Jr (2003) Chemosensitivity linked to p73 function. *Cancer Cell* **3**, 403–410.

12 Lissy NA, Davis PK, Irwin M, Kaelin WG Jr & Dowdy SF (2000) A common E2F-1 and p73 pathway mediates cell death induced by TCR activation. *Nature* **407**, 642–645.

13 Irwin M, Marin MC, Phillips AC, Seelan RS, Smith DI, Liu W, Flores ER, Tsai KY, Jacks T, Vousden KH *et al.* (2000) Role for the p53 homologue p73 in E2F-1-induced apoptosis. *Nature* **407**, 645–648.

14 Stiewe T & Pützer BM (2000) Role of the p53-homologue p73 in E2F1-induced apoptosis. *Nat Genet* **26**, 464–469.

15 Pozniak CD, Radinovic S, Yang A, McKeon F, Kaplan DR & Miller FD (2000) An anti-apoptotic role for the p53 family member, p73, during developmental neuron death. *Science* **289**, 304–306.

16 Ikawa S, Nakagawara A & Ikawa Y (1999) p53 family genes: structural comparison, expression and mutation. *Cell Death Differ* **6**, 1154–1161.

17 Flores ER, Sengupta S, Miller JB, Newman JJ, Bronson R, Crowley D, Yang A, McKeon F & Jacks T (2005) Tumor predisposition in mice mutant for p63 and p73: evidence for broader tumor suppressor functions for the p53 family. *Cancer Cell* **7**, 363–373.

18 Flores ER, Tsai KY, Crowley D, Sengupta S, Yang A, McKeon F & Jacks T (2002) p63 and p73 are required for p53-dependent apoptosis in response to DNA damage. *Nature* **416**, 560–564.

19 Nakagawa T, Takahashi M, Ozaki T, Watanabe Ki K, Todo S, Mizuguchi H, Hayakawa T & Nakagawara A (2002) Autoinhibitory regulation of p73 by Delta Np73 to modulate cell survival and death through a p73-specific target element within the Delta Np73 promoter. *Mol Cell Biol* **22**, 2575–2585.

20 Blyth K, Cameron ER & Neil JC (2005) The RUNX genes: gain or loss of function in cancer. *Nat Rev Cancer* **5**, 376–387.

21 Ito Y (2008) RUNX genes in development and cancer: regulation of viral gene expression and the discovery of RUNX family genes. *Adv Cancer Res* **99**, 33–76.

22 Anglin I & Passaniti A (2004) Runx protein signaling in human cancers. *Cancer Treat Res* **119**, 189–215.

23 Komori T, Yagi H, Nomura S, Yamaguchi A, Sasaki K, Deguchi K, Shimizu Y, Bronson RT, Gao YH, Inada M *et al.* (1997) Targeted disruption of Cbfa1 results in a complete lack of bone formation owing to maturational arrest of osteoblasts. *Cell* **89**, 755–764.

24 Otto F, Thornell AP, Crompton T, Denzel A, Gilmour KC, Rosewell IR, Stamp GW, Beddington RS, Mundlos S, Olsen BR *et al.* (1997) Cbfa1, a candidate gene for cleidocranial dysplasia syndrome, is essential for osteoblast differentiation and bone development. *Cell* **89**, 765–771.

25 Takahashi A, Satake M, Yamaguchi-Iwai Y, Bae SC, Lu J, Maruyama M, Zhang YW, Oka H, Arai N, Arai K *et al.* (1995) Positive and negative regulation of granulocyte-macrophage colony-stimulating factor promoter activity by AML1-related transcription factor, PEBP2. *Blood* **86**, 607–616.

26 Okuda T, van Deursen J, Hiebert SW, Grosveld G & Downing JR (1996) AML1 the target of multiple chromosomal translocations in human leukemia, is essential for normal fetal liver hematopoiesis. *Cell* **84**, 321–330.

27 Taniuchi I, Osato M, Egawa T, Sunshine MJ, Bae SC, Komori T, Ito Y & Littman DR (2002) Differential requirements for Runx proteins in CD4 repression and epigenetic silencing during T lymphocyte development. *Cell* **111**, 621–633.

28 Li QL, Ito K, Sakakura C, Fukamachi H, Inoue K, Chi XZ, Lee KY, Nomura S, Lee CW, Han SB *et al.* (2002) Causal relationship between the loss of RUNX3 expression and gastric cancer. *Cell* **109**, 113–124.

29 Liu W, Toyosawa S, Furuichi T, Kanatani N, Yoshida C, Liu Y, Himeno M, Narai S, Yamaguchi A & Komori T (2001) Overexpression of Cbfa1 in osteoblasts inhibits osteoblast maturation and causes osteopenia with multiple fractures. *J Cell Biol* **155**, 157–166.

30 Welch RD, Jones AL, Bucholz RW, Reinert CM, Tjia JS, Pierce WA, Wozney JM & Li XJ (1998) Effect of recombinant human bone morphogenetic protein-2 on fracture healing in a goat tibial fracture model. *J Bone Miner Res* **13**, 1483–1490.

31 Karsenty G (1999) The genetic transformation of bone biology. *Genes Dev* **13**, 3037–3051.

32 Vaillant F, Blyth K, Terry A, Bell M, Cameron ER, Neil J & Stewart M (1999) A full-length Cbfa1 gene product perturbs T-cell development and promotes lymphomagenesis in synergy with myc. *Oncogene* **18**, 7124–7134.

33 Browne G, Nesbitt H, Ming L, Stein GS, Lian JB, McKeown SR & Worthington J (2012) Bicalutamide-induced hypoxia potentiates RUNX2-mediated Bcl-2 expression resulting in apoptosis resistance. *Br J Cancer* **107**, 1714–1721.

34 Kayed H, Jiang X, Keleg S, Jesnowski R, Giese T, Berger MR, Esposito I, Löhr M, Friess H & Kleeff J (2007) Regulation and functional role of the Runt-related transcription factor-2 in pancreatic cancer. *Br J Cancer* **97**, 1106–1115.

35 Endo T, Ohta K & Kobayashi T (2008) Expression and function of Cbf a-1/Runx2 in thyroid papillary carcinoma cells. *J Clin Endocrinol Metab* **93**, 2409–2412.

36 Onodera Y, Miki Y, Suzuki T, Takagi K, Akahira J, Sakyu T, Watanabe M, Inoue S, Ishida T, Ohuchi N *et al.* (2010) Runx2 in human breast carcinoma: its potential roles in cancer progression. *Cancer Sci* **101**, 2670–2675.

37 Sase T, Suzuki T, Miura K, Shiiba K, Sato I, Nakamura Y, Takagi K, Onodera Y, Miki Y, Watanabe M *et al.* (2012) Runt-related transcription factor 2 in human colon carcinoma: a potent prognostic factor associated with estrogen receptor. *Int J Cancer* **131**, 2284–2293.

38 Ozaki T, Wu D, Sugimoto H, Nagase H & Nakagawara A (2013) Runt-related transcription factor 2 (RUNX2) inhibits p53-dependent apoptosis through the collaboration with HDAC6 in response to DNA damage. *Cell Death Dis* **4**, e610.

39 Gong JG, Costanzo A, Yang HQ, Melino G, Kaelin WG Jr, Levrero M & Wang JY (1999) The tyrosine kinase c-Abl regulates p73 in apoptotic response to cisplatin-induced DNA damage. *Nature* **399**, 806–809.

40 Agami R, Blandino G, Oren M & Shaul Y (1999) Interaction of c-Abl and p73alpha and their collaboration to induce apoptosis. *Nature* **399**, 809–813.

41 Yuan ZM, Shioya H, Ishiko T, Sun X, Gu J, Huang YY, Lu H, Kharbanda S, Weichselbaum R & Kufe D (1999) p73 is regulated by tyrosine kinase c-Abl in the apoptotic response to DNA damage. *Nature* **399**, 814–817.

42 Costanzo A, Merlo P, Pediconi N, Fulco M, Sartorelli V, Cole PA, Fontemaggi G, Fanciulli M, Schiltz L, Blandino G *et al.* (2002) DNA damage-dependent acetylation of p73 dictates the selective activation of apoptotic target genes. *Mol Cell* **9**, 175–186.

43 Wang CQ, Jacob B, Nah GS & Osato M (2010) Runx family genes, niche, and stem cell quiescence. *Blood Cells Mol Dis* **44**, 275–286.

44 McGee-Lawrence ME, Li X, Bledsoe KL, Wu H, Hawse JR, Subramaniam M, Razidlo DF, Stensgard BA, Stein GS, van Wijnen AJ *et al.* (2013) Runx2 protein represses Axin2 expression in osteoblasts and is required for craniosynostosis in Axin2-deficient mice. *J Biol Chem* **288**, 5291–5302.

45 Fontemaggi G, Gurtner A, Strano S, Higashi Y, Sacchi A, Piaggio G & Blandino G (2001) The transcriptional repressor ZEB regulates p73 expression at the crossroad between proliferation and differentiation. *Mol Cell Biol* **21**, 8461–8470.

46 Bui T, Sequeira J, Wen TC, Sola A, Higashi Y, Kondoh H & Genetta T (2009) ZEB1 links p63 and p73 in a novel neuronal survival pathway rapidly induced in response to cortical ischemia. *PLoS One* **4**, e4373.

47 Aghdassi A, Sendler M, Guenther A, Mayerle J, Behn CO, Heidecke CD, Friess H, Büchler M, Evert M, Lerch MM *et al.* (2012) Recruitment of histone deacetylases HDAC1 and HDAC2 by the transcriptional repressor ZEB1 downregulates E-cadherin expression in pancreatic cancer. *Gut* **61**, 439–448.

48 Rödicker F & Pützer BM (2003) p73 is effective in p53-null pancreatic cancer cells resistant to wild-type TP53 gene replacement. *Cancer Res* **63**, 2737–2741.

49 Willis AC, Pipes T, Zhu J & Chen X (2003) p73 can suppress the proliferation of cells that express mutant p53. *Oncogene* **22**, 5481–5495.

50 Chen X, Zheng Y, Zhu J, Jiang J & Wang J (2001) p73 is transcriptionally regulated by DNA damage, p53, and p73. *Oncogene* **20**, 769–774.

Cancer Science

Identification of a novel E-box binding pyrrole-imidazole polyamide inhibiting MYC-driven cell proliferation

Rajeev Mishra,[1,2] Takayoshi Watanabe,[1,3] Makoto T. Kimura,[1] Nobuko Koshikawa,[3] Maki Ikeda,[1] Shota Uekusa,[1] Hiroyuki Kawashima,[1,4] Xiaofei Wang,[1] Jun Igarashi,[1] Diptiman Choudhury,[2] Carla Grandori,[5] Christopher J. Kemp,[5] Miki Ohira,[3] Narendra K. Verma,[6] Yujin Kobayashi,[7] Jin Takeuchi,[7] Tsugumichi Koshinaga,[4] Norimichi Nemoto,[8] Noboru Fukuda,[9] Masayoshi Soma,[10] Takeshi Kusafuka,[4] Kyoko Fujiwara[10] and Hiroki Nagase[1,3]

[1]Division of Cancer Genetics, Department of Advanced Medical Science, Nihon University Research Institute of Medical Science, Tokyo, Japan; [2]Department of Medicine, Cedars-Sinai Medical Center, Samuel Oschin Comprehensive Cancer Institute, Los Angeles, California, USA; [3]Chiba Cancer Center Research Institute, Chiba; [4]Division of Pediatric Surgery, Department of Surgery, Nihon University Research Institute of Medical Science, Tokyo, Japan; [5]Division of Human Biology, Fred Hutchinson Cancer Research Center, Seattle, Washington, USA; [6]Department of Biological Sciences, Padova University, Padova, Italy; [7]Division of Hematology, Department of Internal Medicine, Nihon University Research Institute of Medical Science, Tokyo; [8]Department of Pathology and Microbiology, Nihon University Research Institute of Medical Science, Tokyo; [9]Life Science, Advanced Research Institute for the Sciences and Humanities, Nihon University, Tokyo; [10]Innovative Therapy Research Group, Nihon University Research Institute of Medical Science, Tokyo, Japan

The MYC transcription factor plays a crucial role in the regulation of cell cycle progression, apoptosis, angiogenesis, and cellular transformation. Due to its oncogenic activities and overexpression in a majority of human cancers, it is an interesting target for novel drug therapies. MYC binding to the E-box (5'-CAC-GTGT-3') sequence at gene promoters contributes to more than 4000 MYC-dependent transcripts. Owing to its importance in MYC regulation, we designed a novel sequence-specific DNA-binding pyrrole–imidazole (PI) polyamide, Myc-5, that recognizes the E-box consensus sequence. Bioinformatics analysis revealed that the Myc-5 binding sequence appeared in 5'- MYC binding E-box sequences at the eIF4G1, CCND1, and CDK4 gene promoters. Furthermore, ChIP coupled with detection by quantitative PCR indicated that Myc-5 has the ability to inhibit MYC binding at the target gene promoters and thus cause downregulation at the mRNA level and protein expression of its target genes in human Burkitt's lymphoma model cell line, P493.6, carrying an inducible MYC repression system and the K562 (human chronic myelogenous leukemia) cell line. Single i.v. injection of Myc-5 at 7.5 mg/kg dose caused significant tumor growth inhibition in a MYC-dependent tumor xenograft model without evidence of toxicity. We report here a compelling rationale for the identification of a PI polyamide that inhibits a part of E-box-mediated MYC downstream gene expression and is a model for showing that phenotype-associated MYC downstream gene targets consequently inhibit MYC-dependent tumor growth.

The transcription factor c-MYC possesses an exclusive and extensive set of biological actions that underlie its role as a salient oncogene and therefore could be the key to anticancer drug development. The c-MYC proto-oncogene belongs to the family of MYC genes that includes B-MYC, L-MYC, N-MYC, and S-MYC.[1] Among them, c-MYC (here after referred as MYC) is found in almost all proliferating cells and expression of N- and L-MYC is more constrained to specific cell types.[2] MYC is a basic helix–loop–helix leucine zipper transcription factor that binds DNA in a sequence-specific manner[3] and activates the transcription of genes whose products are involved in crucial aspects of cancer biology such as cell proliferation, cell growth, apoptosis, and differentiation.[4] The biological activities of MYC depends on its ability to heterodimerize with its protein partner, MAX, to bind the enhancer box (E-box) sequence and stimulate transcription of a number of its downstream genes.[4,5] The MAX:MAX homodimer or MAD:MAX heterodimer is supposed to antagonize the functions of MYC by binding to the same core E-box sequences.[6]

MYC targets approximately 10–15% of all cellular promoters in human cells, which is higher than any other typical transcription factor.[7] Target genes of MYC identified in mammalian cells include genes involved in cell cycle, ribosomal biogenesis, protein synthesis, and mitochondrial function.[4,5,8] Among the direct target genes of MYC, those with E-box binding sites include *ODC*, *ECA39*, *eIF4E*, *CDC25*, *CAD*, *CDK4*, *eIF4G1*, and *CCND1*.[9,10] MYC has been known to play a crucial role in malignant transformation.[11] Several attempts have been made using small molecule inhibitors to inhibit MYC binding at gene promoters.[11–15] Pyrrole–imidazole (PI) polyamides are a class of sequence-specific DNA-binding small molecules that have been shown to be effective inhibitors of transcription factors by disrupting essential

protein–DNA interactions.[16–20] Our group and others have designed PI polyamides to specifically target critical regulatory proteins, including MMP-9, transforming growth factor-β1, vascular endothelial growth factor, hypoxia-inducible factor 1-α, androgen receptor, epidermal growth factor receptor, prostate-specific antigen, and lectin-type oxidized LDL receptor-1.[16,21–24] Recently, we have demonstrated that E-Box recognizing PI polyamide, Myc-6 was found to significantly suppress malignant phenotypes of human osteosarcoma MG63 cells both *in vitro* and *in vivo*, showing the potential of PI polyamides in cancer therapy.[25]

In the present study, we developed an E-box-binding PI polyamide, Myc-5 (target sequence 5'-WCWCGWGW-3', where W = A or T) to inhibit MYC target genes. Myc-5 showed inhibition of MYC-driven cell growth by downregulation of a subgroup of MYC downstream genes, including *eIF4GI* and *CCND1*, at an early stage of transcription. In animal tumor model studies, Myc-5 inhibits tumor growth by inhibiting cell proliferation and inducing apoptosis in tumor tissue. Collectively, our results establish a transcriptional regulation at an early stage of MYC regulatory proteins by using PI polyamides and provide a novel antitumor agent targeting MYC function.

Materials and Methods

Cell culture. The human Burkitt's lymphoma model cell line, P493.6, carrying Tet-repressible c-MYC system and chronic myeloid leukemia cell line K562, were used in this study. To suppress MYC expression, P493.6 cells were treated with 0.1 μg/mL tetracycline for 3 days before treatment with Myc-5. The P493.6 cell line was kindly provided by C. Grandori (Fred Hutchinson Cancer Research Center, Seattle, WA, USA) and K562 cells were obtained from the Riken cell bank (Ibaraki, Japan).

Synthesis of PI polyamides targeting the E-box consensus sequence. Myc-5 was designed to target the E-box consensus sequence and mismatch PI polyamide was designed to target by exchanging the CG dinucleotide with GC in the center of

the E-box (Fig. 1a,c). Fluorescein isothiocyanate-conjugated Myc-5 was also synthesized for nuclear localization experiments (Fig. 1b). All of the PI polyamides were synthesized according to previously established methods.[21]
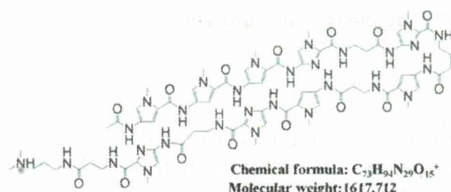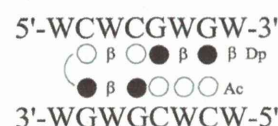
Electrophoretic mobility shift assay and surface plasmon resonance. FITC-labeled matching hairpin oligonucleotide (46 base pair) corresponding to eIF4G1 gene promoters having E-box consensus binding sites and mismatch promoter were synthesized (Table S1) for EMSA. Results were visualized by luminescent image analyzer LAS3000 (Fujifilm, Tokyo, Japan). The kinetic measurements of the polyamides' binding curves to the biotin-labeled double-stranded DNA (having the E-box consensus sequence) and data processing were carried out on a Biacore 2000 system as described previously.[26]

Quantitative real-time PCR. Total RNA was extracted and digested with DNase I using the RNeasy kit according to the manufacturer's protocol (Qiagen, Valencia, CA, USA). The primer sequences are listed in Table S2. Relative gene expression was determined by normalizing the gene expression of each target gene to *GAPDH*.
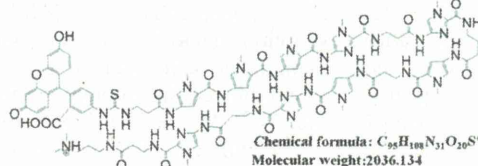
Conventional ChIP followed by real-time PCR. The status of polyamide binding at the target promoter region (Table S3) was detected using a ChIP assay kit (Upstate Biotechnology, Upstate Biotechnology, Inc., Lake Placid, NY, USA) following the manufacturer's protocol. ChIP DNA was further analyzed by quantitative PCR using primers encompassing the regions of interest on the eIF4G1, CCND1, and CDK4 promoters.

Tumorigenicity studies in SCID mice. Seven-week-old SCID mice were housed under specific pathogen-free conditions. Experiments were approved by the committee for laboratory animal welfare and ethics of Nihon University School of Medicine (Tokyo, Japan). The effect of Myc-5 on the xenograft model was examined as follows. P493.6 cells (1×10^7) were inoculated s.c. into the flank of mice and they were divided into three treatment groups: control group (PBS i.v.; $n = 8$); a Myc-5 treated group (7.5 mg/kg i.v., single dose; $n = 8$); and a doxycycline treated group (0.01% doxycycline in regular
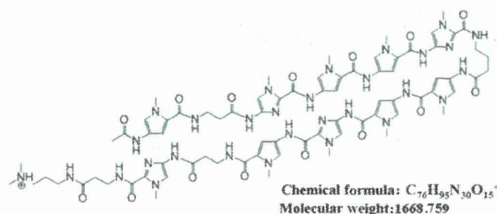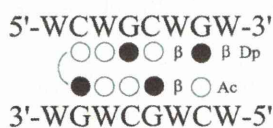
(a) Myc-5

5'-WCWCGWGW-3'

3'-WGWGCWCW-5'

Chemical formula: $C_{73}H_{94}N_{29}O_{15}{}^+$
Molecular weight: 1617.712

(b) FITC-Myc-5

Chemical formula: $C_{95}H_{108}N_{31}O_{20}S^+$
Molecular weight: 2036.134

(c) Mismatch PI

5'-WCWGCWGW-3'

3'-WGWCGWCW-5'

Chemical formula: $C_{76}H_{95}N_{30}O_{15}{}^+$
Molecular weight: 1668.759

Fig. 1. Designed pyrrole–imidazole (PI) polyamide structure and binding site. Structures and binding sites for synthesized PI polyamides Myc-5 (a), FITC-labeled Myc-5 (b), and mismatch PI polyamide (c). Base sequence specificity depends on side-by-side pairing of pyrrole and imidazole amino acids in the minor groove of DNA. Black and white circles represent imidazole and pyrrole rings, respectively; curved lines represent hairpin junctions. β, β-alanine; Dp, diaminomethylene propylamide; W, A or T.

drinking water; $n = 5$). Doxycycline induces repression of P493.6 xenograft tumor growth in a MYC-dependent manner. The treatment was started on day 7 after cell inoculation and mice were killed after 30 days of treatment.

In vivo **nuclear localization.** For *in vivo* nuclear localization analysis by fluorescence microscopy, tumor-bearing mice were injected with FITC-labeled Myc-5 (0.15 mg) into the lateral tail vein of the animals. Tumor tissues, along with adjacent normal tissues, were collected 5 days after the injection for analysis using propidium iodide as a nuclear dye to identify nucleated cells.

Statistical analysis. Results are shown as mean ± SD. Each experiment was carried out independently three times. The level of significance (**$P < 0.05$ and ***$P < 0.001$) was determined using Student's *t*-test.

Additional supplementary materials and methods detailing cell viability assay, detection of nuclear localization by confocal microscopy, histopathology, Western blot analysis, microarray analyses, and references can be found in Documents S1 and S2.

Results

Identification of MYC target genes that harbor Myc-5 consensus sequence. E-boxes are present in many genes, but not all are known to be direct transcriptional targets of MYC. Based on compilations by Fernandez *et al.*,[27] we found that 105 genes harbor the Myc-5 binding site (WCWCGWGW) in their E-box consensus sequence (Table S4). These genes can be classified into a wide range of functional classes. Here we focused on genes related to translation and proliferation. Among the ten top MYC-regulated genes we chose two proliferation genes (*CDK4* and *CCND1*) and a translation gene (*eIF4G1*). The selected genes have been well characterized by previous researchers and are also well known direct targets of MYC.[9,10,28]

DNA-binding affinity and specificity of designed Myc-5 PI polyamide. The EMSA and surface plasmon resonance (SPR) assay are used to determine the binding affinity and specificity of PI polyamide to its target DNA. The EMSA results demonstrated that a clear mobility band shift (Fig. 2a,b) was detected when Myc-5 was incubated with eIF4G1 gene promoter oligonucleotide, whereas no shift was detected for the mismatch PI polyamide (Fig. 2a, lane 4) or eIF4G1 mismatch gene promoter (Fig. 2a, lane 5) in which the core recognition sequence, CACGTG, was replaced by CAGCTG. Increasing concentrations of Myc-5, but not of the mismatch PI polyamide, bound to the eIF4G1 promoter oligo (Fig. 2b, lanes 2–5), suggesting that Myc-5 can specifically bind to sequences of their target gene-promoters. To further confirm binding of the E-box to
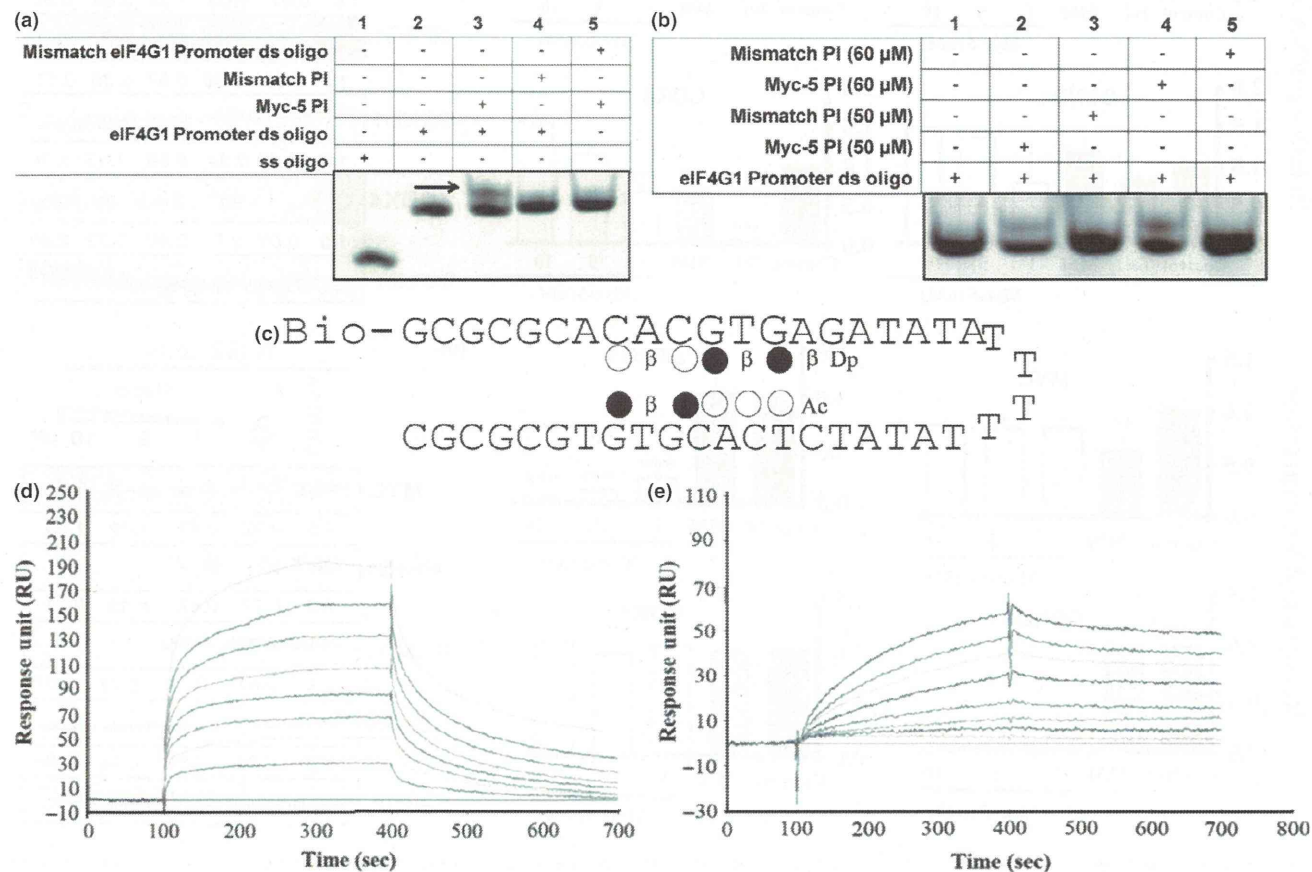

Fig. 2. Myc-5 binding at the target gene promoters. (a) EMSA of *eIF4G1* gene match and mismatch promoter and with Myc-5 and mismatch pyrrole–imidazole (PI) polyamide. (b) EMSA of *eIF4G1* gene promoter with Myc-5 and mismatch PI polyamide. FITC-labeled hairpin oligonucleotide was incubated at 37°C for 60 min in Myc-5 or mismatch PI polyamide. (c) Typical surface plasmon resonance sensograms for the interaction between PI polyamides and the hairpin duplex with 5′-biotin labeled and immobilized E-box (CACGTG) sequences. (d, e) Remarkable differences in binding kinetics were observed: fast on/off kinetics for Myc-5 (d), and slower kinetics for the mismatch PI polyamide (e).

the target gene promoter, we used a biosensor-SPR assay to explore the interaction of Myc-5 with biotinylated hairpin duplexes having WCWCGWGW sequences (Fig. 2c). The kinetic profile of Myc-5 revealed a relatively fast "on-rate" and slow "off-rate" in binding with a K_D of $4.81 \pm 2.79 \times 10^{-8}$ M. The mismatch PI polyamide showed slow "on-rate" and fast "off-rate" with K_D was calculated at $5.1 \pm 0.54 \times 10^{-5}$. In summary, these results confirm that the presence of the E-box in the DNA sequence has a pronounced influence on the binding of Myc-5 and yields a 654-times higher affinity than the mismatch PI polyamide (Fig. 2d,e, Table S5).

Myc-5 inhibited cell proliferation and localized into nucleus in P493.6 and K562 cell lines. P493.6 and K562 cells were incubated with different concentrations (1–10 μM) of Myc-5 and mismatch PI polyamide and viability was determined at 24, 48, and 72 h after treatment, respectively. As shown in Figure

S1, cell viability was significantly reduced ($P < 0.001$ vs control) in both cell lines treated with Myc-5 in a time- and concentration-dependent manner. Nuclear localization of Myc-5 was determined by FITC-conjugated Myc-5 using laser confocal fluorescence microscopy. Green fluorescence indicates the presence of Myc-5 and red fluorescence depicts the cell nuclei, indicating that Myc-5 localizes into nuclei within 2 h (Fig. S2a,c,d). In contrast, cells incubated with FITC solution (control) at the same concentration did not localize into nuclei (Fig. S2b) in either cell line.

Myc-5 attenuates MYC binding at the gene promoter, causing downregulation of MYC target genes. Myc-5 inhibited target gene expression at protein and mRNA levels (Fig. 3a,b). Cells treated with Myc-5 at 10 μM concentration for 72 h caused statistically significant suppression of eIF4G1 mRNA compared with control or mismatch PI polyamide treated cells in both systems. The CCND1 mRNA was unaffected in
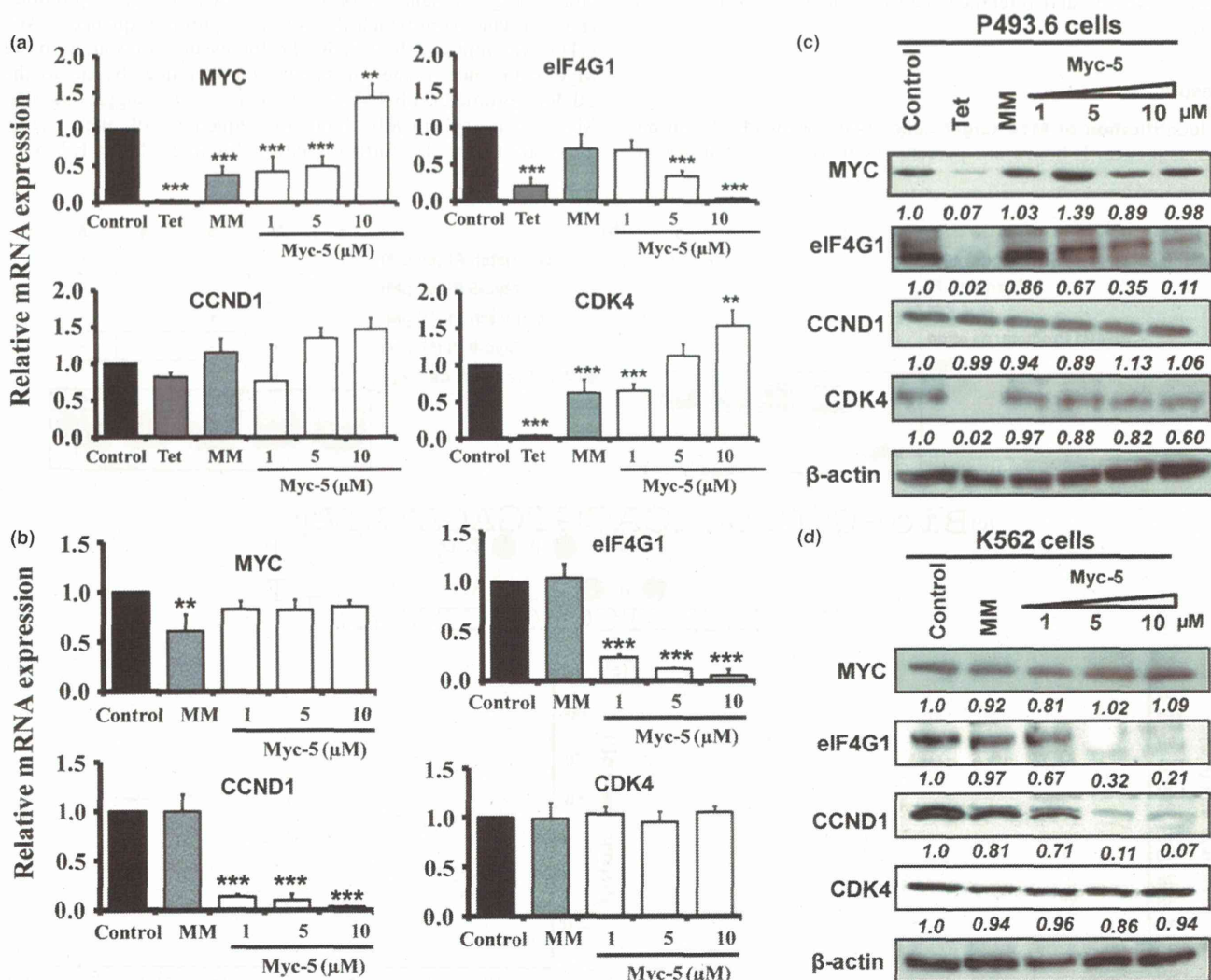
Fig. 3. Myc-5 downregulates mRNA expression and protein expression of target genes. (a, b) Expression of target genes was detected by quantitative real-time PCR after 72 h of treatment with control, Myc-5 (1, 5, and 10 μM concentration), or mismatch PI polyamide (MM) at 10 μM concentration and normalized with GAPDH in P493.6 (a) and K562 (b) cells. Data are shown as mean values with error bars representing ±SD. Statistical significance was calculated by Student's t-test. **$P < 0.05$, ***$P < 0.001$ when compared to control. (c, d) P493.6 and K562 cells were treated with Myc-5 (1, 5, and 10 μM) or mismatch PI polyamide (10 μM; MM) for 72 h. β-actin was used as the loading control. The relative band intensities in P493.6 and K562 cells were determined by dividing the intensity of the band by β-actin followed by normalization to the control. Tet, tetracycline.

all treated and untreated groups of P493.6 cells; however, its expression was significantly ($P < 0.001$) downregulated in the K562 cell line compared to control and mismatch PI polyamide treated groups. The mRNA expression correlated well with protein expression in the Myc-5 administration using both cell systems (Fig. 3c,d). To investigate whether target gene expression is directly regulated by Myc-5, we used ChIP assays of the E-box and exonic region (Figs 4a,b, S3a). The exonic region was taken as an arbitrary negative control region during the analysis. The ChIP analysis revealed that, compared to control, the Myc-5 and tetracycline groups significantly inhibited binding of MYC to the E-box region in P493.6 cells (Figs 4c,S3b) at the eIF4G1 and CDK4 gene promoters. In contrast, the E-box and control regions (exon) of CCND1 gene promoter showed restrained enrichment in all treated groups (Fig. 4d). Similarly, MYC was specifically enriched near the E-box site at the eIF4G1, CCND1, and CDK4 gene promoters but not in the Myc-5 treated group in K562 cells (Figs 4e,f,S3c). Moreover, our microarray analysis results showed (Fig. S4a,b) that differentially expressed genes in K562 cells (29 upregulated and 21 downregulated) and P943.6 cells (20 genes upregulated and 20 downregulated) were identified by unpaired two-

class significance analysis of microarray with 0% false discovery rate. Among the top 50 modulated genes, five were carrying the Myc-5 consensus sequence in their promoter, as identified from Table S4.

Myc-5 retards growth in animal tumor models. To investigate whether the *in vitro* efficacy of Myc-5 can also be recapitulated *in vivo*, therapeutic animal studies were carried out using P493.6 s.c. xenografts. Mice were inoculated s.c. with P493.6 (high MYC expressing) cells. One week after inoculating the cells, when the tumor volumes reached approximately 100 mm³, mice were split into three groups and treated with either saline, doxycycline, or 7.5 mg/kg Myc-5 injected i.v. into the lateral tail vein of animals at day 7 (single dose; Fig. 5a). Myc-5 was formulated based on previous xenograft studies with PI polyamide.[20,29,30] Growth curve data indicated that Myc-5 (7.5 mg/kg) and doxycycline treated groups had a significantly smaller tumor volume during the growth phase ($P < 0.001$ *vs* control; Fig. 5b) by the end of the study. Representative images of each group of mice are shown in Fig. 5b (inset). All mice with Myc-5 treatment continued to gain weight at an equal rate throughout the treatment period (Fig. 5c). The average tumor weight results further confirmed inhibition of tumor growth as Myc-5 and doxycycline treated groups
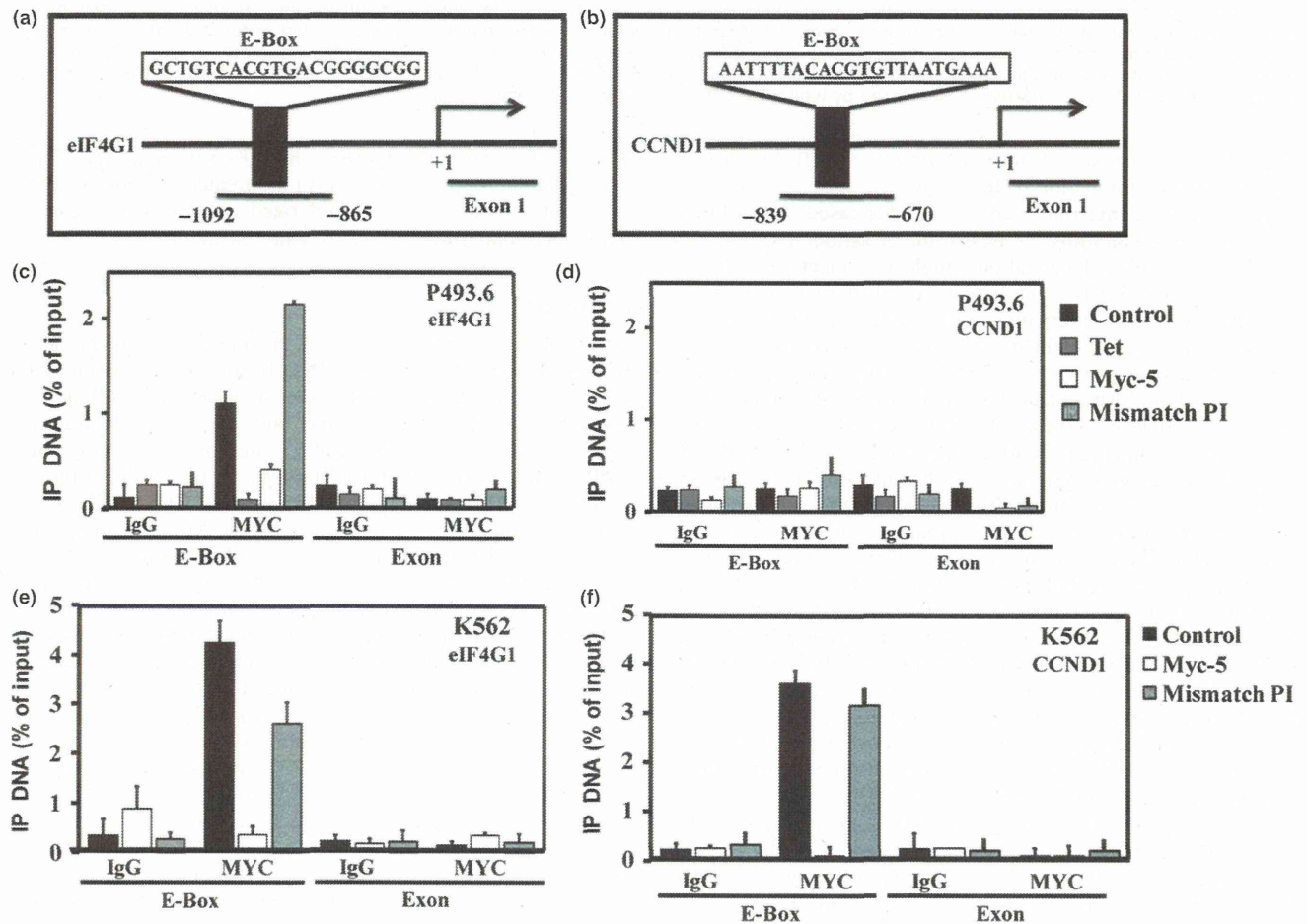

Fig. 4. *In vivo* binding of Myc-5 to the E-box at its target gene promoter. (a, b) Schematic depiction of the Myc-5 target gene promoter with MYC binding site (underline) indicated. (c–f) ChIP assay of Myc-5 target genes in the P493.6 (c, d) and K562 (e, f) cell systems. Labeled regions (E-box and exon) of each gene were quantitatively amplified by real-time PCR. Data are representative of three independent experiments. Tet, tetracycline.
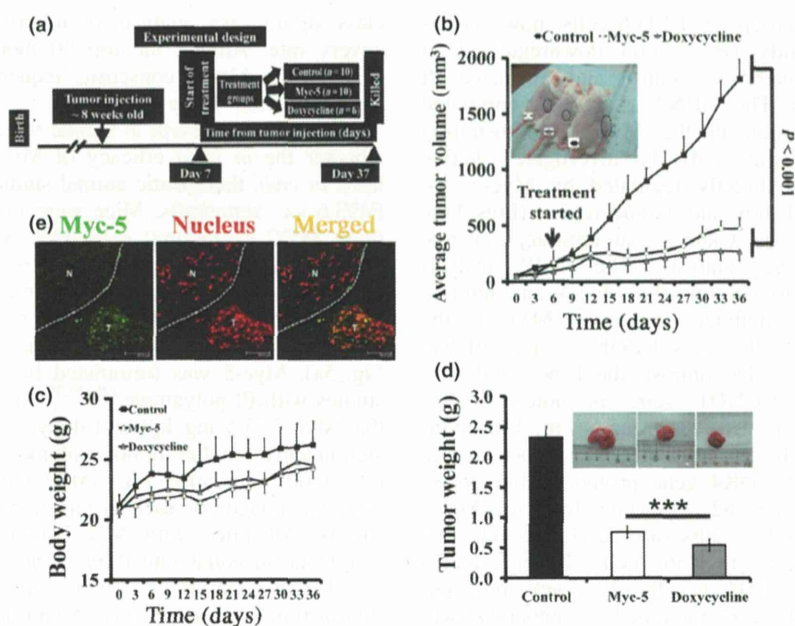
Fig. 5. Myc-5 blocks the growth of P493.6 xenografts. (a) Schematic diagram of the xenograft model illustrating timing of tumor implantation and treatment. Eight-week-old SCID mice were s.c. injected with P493.6 cells. (b) Tumor growth chart showing the effect of treatment *in vivo*. Myc-5 (7.5 mg/kg) and doxycycline significantly slowed tumor growth ($P < 0.001$) at the termination point in comparison to the control group. Representative picture shows each group of mice (inset). (c) Mean body weight for each treatment group plotted as function of day after post-injection. (e) Comparisons of excised tumor weights for three different treatment groups at the end of study. Data in (b, d, e) are shown as the mean ± SD. Statistical significance was calculated by Student's *t*-test. ***$P < 0.001$. (e) FITC-labeled Myc-5 localizes to nucleus of P493.6 xenograft leaving normal tissue unaffected (separated by white line). N: Normal tissue, T: tumor tissue.

were found to be significantly lower ($P < 0.001$ vs control; Fig. 5d) at the termination of the study.

Myc-5 localizes into tumor and causes decreased cell proliferation and induced apoptosis in P493.6 tumor xenografts. To evaluate *in vivo* nuclear localization, single i.v. injection of FITC-conjugated Myc-5 was given to P493.6 cell-derived xenografts. Twenty-four hours after injection, animals were killed and tumor tissues were obtained. The tumor-derived tissues were found to display strong and characteristic nuclear staining (Fig. 5e). In contrast, adjacent normal tissues were found to be devoid of nuclear fluorescence (Fig. 5e). Myc-5 was found throughout the tumor, indicating its capacity to enter the tumor through the vascular system. To assess the activity of Myc-5, tumors were harvested from all treatment groups and examined by histopathology. Microscopic analysis of H&E staining showed that Myc-5 and doxycycline treated tumors showed areas with necrosis, cellular debris, and swollen cells with cytoplasmic vacuoles as compared with the vehicle-treated control (Fig. 6a; left). In order to investigate the mechanism underlying Myc-5-mediated tumor growth inhibition in P493.6 xenografts, immunohistochemical analyses were carried out for BrdU uptake, and TUNEL reaction assay. BrdU-positive nuclei were detected in a small number of cells in Myc-5 treated tumor as compared to control group (Fig 6a; middle). In contrast, a large number of cells stained positively for TUNEL in Myc-5 or doxycycline treated group (Fig. 6a; right) compared to the control group. Quantitative data were consistent with the expression pattern of BrdU and TUNEL staining assays (Fig. 6b). Quantification of BrdU-positive cells in the control group were significantly ($P < 0.001$) reduced (approximately 83% and 76% reductions in Myc-5 and doxycycline groups, respectively) compared to treated groups. The TUNEL analysis showed that the number of apoptotic cells was significantly higher

($P < 0.001$; approximately 38% and 30% higher in Myc-5 and doxycycline groups, respectively) in treated groups. Overall, we found that Myc-5 is well tolerated, inhibits tumor growth, and induces apoptosis in P493.6 xenograft mouse models.

Discussion

In this study, we synthesized two β-alanine-linked polyamides of different lengths: Myc-5 (AcPyPyPyImβImγPyβPyImβImβDp), where Py is pyrrole, Im is imidazole, Ac is acetyl, β is β-alanine, Dp is dimethylaminopropylamine, and γ is γ-*turn* to target the 8-bp site of 5′-WCWCGWGW-3′; and mismatch polyamide (AcPyβImPyPyImγPyPyImPyβImβDp) to target the 8-bp site 5′-WCWGCWGW-3′, flipping dinucleotide CG to GC at the central portion (Fig. 1a,b). A search for Myc-5-binding sites from the published database[27] revealed that the Myc-5 consensus sequence was flanking the E-box of genes involved in apoptosis, cell cycle, nucleolar function, ribosomal proteins, and translation initiation factors. Among them, we focused on the *eIF4G1*, *CCND1*, and *CDK4* genes because they carry a Myc-5 consensus sequence including a MYC binding site (E-box) in the promoter region (Fig. S3d) and their transcription is modulated by MYC.[9,10,28] Using EMSA and Biacore analyses, our results showed that Myc-5 binds specifically and with high affinity (654 times; Table S5) to the eIF4G1, CCND1, and CDK4 gene promoters at the E-box region (Fig. 2). The effective concentration of Myc-5 in the EMSA was higher than the concentration for biological effect, which is consistent with results obtained for other compounds;[31] possibly, PI polyamide accumulates in cells to effectively reach the intracellular and intranuclear levels.[32] The higher binding affinity of Myc-5 in comparison to mismatch PI polyamide might be explained as the targeted PI polyamide has more aliphatic
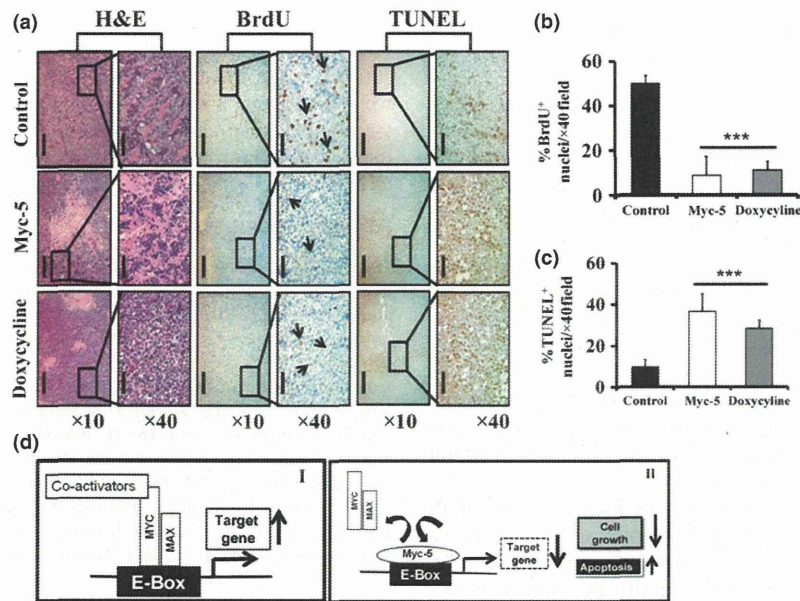
Fig. 6. Histopathology of xenografts in nude mice and illustration of potential mechanism by Myc-5. (a) Tissue sample were analyzed qualitatively for morphological changes. Magnification, ×10 (scale bar = 200 μm); magnification, ×40 (scale bar = 50 μm). (b, c) Quantitative data of immunohistochemical analysis of BrdU and TUNEL positive staining in each group. Data in (b, c) are shown as the mean ± SD of three tumor samples from an individual mouse in each group. Statistical significance was calculated by Student's *t*-test. ***$P < 0.001$. (d) Schematic diagram of the mechanism by which pyrrole–imidazole polyamide inhibits MYC/MAX interaction to the E-box. (I) MYC:MAX dimer binds to E-box and activates MYC target gene expression. (II) Myc-5 occupied the E-box by binding, thereby inhibiting the MYC/MAX interaction to the E-box, causing further suppression of target gene expression.

β-alanine unit, giving it more flexibility and optimizing the positioning of the imidazole amino acids on binding to its targeted sequence.[33] *In vivo* binding of Myc-5 to their target gene-promoter was confirmed by ChIP assay. Results of ChIP indicated that MYC transcription factor bound E-box in the control group whereas, in treated groups, Myc-5 inhibited MYC binding on its target gene promoters. However, in the P493.6 cell line, the CCND1 gene-promoter showed only a background signal that was obtained at the E-box region as well as in the control (exon) regions (Fig. 4d). These results were consistent with previous reports of the absence of this regulator in the B cell line.[34]

Myc-5 was used at the concentration of 10 μM based on previous studies using PI polyamides.[19,20,35] Myc-5 significantly reduced mRNA and protein expression of MYC target genes at this given concentration. The correlation between MYC binding and mRNA expression of Myc-5 was established by real-time mRNA expression analysis and Western blot analysis. The *eIF4G1* gene has a downregulated expression and might be a direct target of MYC in both systems, which was also favored by EMSA and ChIP data. CCND1 mRNA expression was downregulated in the K562 cell line with Myc-5 treatment in a dose-dependent manner, which is known to exert positive growth effects and to be regulated by MYC.[36] The mRNA expression of *CDK4*, a positive growth controller of MYC,[28] was unaffected by Myc-5 treatment as the Myc-5 binding site (E-box#2) has no role in MYC-dependent gene regulation.[28] We analyzed the CDK4 promoter region for putative MYC binding sites. Our sequence analysis revealed the presence of four E-box sequences, which could be recognized by MYC (Fig. S2). Among them, only E-box#2 is a putative binding site for Myc-5 as it contains the Myc-5 consensus sequence. As shown in Figure S2, Myc-5 bound to the E-box#2 of the CDK4 promoter. The *CDK4* gene is

established as a direct target of MYC identified by serial analysis of gene expression with essential E-boxes in their promoters.[28] The CDK4 promoter contains four highly conserved E-box elements where E-box#3 and #4 were the most important for CDK4 promoter activity.[28] The Myc-5 effect on mRNA expression of the MYC gene and further its transcriptional target genes were analyzed by real-time PCR in K562 and P493.6 cell lines. In K562 cells, MYC mRNA expression is unaffected by Myc-5 treatment and a similar trend was observed in its target gene CDK4 mRNA expression. However MYC mRNA expression in Myc-5 treated group is significantly increased as compared to control group in P493.6 cells. P493.6 B lymphoma cells overexpress MYC, which indicates that P493.6 cell lines may have some mutations on its promoter or regulator regions. The MYC promoter or regulatory regions do not have any Myc-5 binding consensus sequence. This may be due to some specific mutation in these regions that might have generated a novel Myc-5 binding site at the MYC promoter of P493.6 cells. This novel Myc-5 binding site in the promoter could be acting as a transcriptional activator of the MYC gene and helping it to further overexpress. Furthermore, Myc-5 has very high affinity for its consensus sequence and may act as a non-competitive inhibitor of MYC protein. Therefore, overexpression of MYC protein in P493.6 cells does not have an effect on MYC downstream genes with active Myc-5 binding sites, such as eIF4G1.

Taken together, our data are compatible with a mechanism that involves the recruitment of Myc-5 at E-box sites within the promoter of the MYC target gene, thereby inhibiting MYC binding at particular sites and inhibiting target gene function instead of blocking MYC. Myc-5 downregulates its target gene transcription, supporting the notion that polyamides bind to DNA with affinity and sequence-specificity comparable to DNA-binding proteins and gene expression can be regulated

by competitive displacement of transcription factor from DNA target sequences,[37] where Myc-5 consensus sequences are not contained.

Myc-5 exerts its therapeutic role in tumor maintenance through selective effects on the translation of specific downstream genes. In our *in vivo* study we used 7.5 mg/kg on the basis of prior pharmacokinetic profiles and previous analytical studies.[26,38] We identified strong *in vivo* nuclear localization of Myc-5 and also its inhibitory effect on tumor growth in a P493.6 mouse model. One possible reason for this activity can be explained by previous reports showing that changes in the levels or activity of eIF4F mediate the translational regulation of specific genes involved (as in the P493.6 cell line, eIF4G1 is completely suppressed) in survival and apoptosis.[39] In nasopharyngeal carcinoma, knockdown of eIF4G1 expression markedly inhibited cell-cycle progression, proliferation, and suppressed *in vivo* xenograft tumor growth,[40,41] which might be applicable to our system as well.

In conclusion, the results reported here identify a novel PI polyamide, Myc-5, as a lead compound targeting against the E-box and thereby modulating expression of some genes. Our approach can be an efficient tool to identify the sequence-specific compound that targets the E-box and specifically modulates MYC downstream genes and interferes with their pathways. Myc-5 competes with the MYC:MAX heterodimer and inhibits transregulation of the target gene promoter (Fig. 6d) at the E-box. The extension of this approach could result in the identification of more potent inhibitory PI polyamides in multiple pathways and reveal a new E-box-regulated target or combination of targets for a distinct MYC function, which may have formidable therapeutic opportunities for the future.

Acknowledgments

Disclosure Statement

The authors have no conflict of interest.

References

1 Adhikary S, Eilers M. Transcriptional regulation and transformation by Myc proteins. *Nat Rev Mol Cell Biol* 2005; **6**: 635–45.
2 Luscher B. Function and regulation of the transcription factors of the Myc /Max/Mad network. *Gene* 2001; **277**: 1–14.
3 Blackwood EM, Eisenman RN. Max: a helix-loop-helix zipper protein that forms a sequence-specific DNA-binding complex with Myc. *Science* 1991; **251**: 1211–7.
4 Dang CV, O'Donnell KA, Zeller KI *et al.* The c-Myc target gene network. *Semin Cancer Biol* 2006; **16**: 253–64.
5 Liu YC, Li F, Handler J *et al.* Global regulation of nucleotide biosynthetic genes by c-Myc. *PLoS One* 2008; **3**: e2722.
6 Ayer DE, Eisenman RN. A switch from Myc: Max to Mad: Max heterocomplexes accompanies monocyte/macrophage differentiation. *Genes Dev* 1993; **7**: 2110–9.
7 Guccione E, Martinato F, Finocchiaro G *et al.* Myc-binding-site recognition in the human genome is determined by chromatin context. *Nat Cell Biol* 2006; **8**: 764–70.
8 Zeller KI, Jegga AG, Aronow BJ *et al.* An integrated database of genes responsive to the Myc oncogenic transcription factor: identification of direct genomic targets. *Genome Biol* 2003; **4**: R69.
9 Huerta M, Munoz R, Tapia R *et al.* Cyclin D1 is transcriptionally down-regulated by ZO-2 via an E box and the transcription factor c-Myc. *Mol Biol Cell* 2007; **18**: 4826–36.
10 Lin CJ, Cencic R, Mills JR *et al.* c-Myc and eIF4F are components of a feedforward loop that links transcription and translation. *Cancer Res* 2008; **68**: 5326–34.
11 Albihn A, Johnsen JI, Henriksson MA. MYC in oncogenesis and as a target for cancer therapies. *Adv Cancer Res* 2010; **107**: 163–224.
12 Wang H, Chauhan J, Hu A *et al.* Disruption of Myc-Max heterodimerization with improved cell-penetrating analogs of the small molecule 10074-G5. *Oncotarget* 2013; **4**: 936–47.
13 Wang H, Hammoudeh DI, Follis AV *et al.* Improved low molecular weight Myc-Max inhibitors. *Mol Cancer Ther* 2007; **6**: 2399–408.
14 Yin X, Giap C, Lazo JS *et al.* Low molecular weight inhibitors of Myc-Max interaction and function. *Oncogene* 2003; **22**: 6151–9.
15 Delmore JE, Issa GC, Lemieux ME *et al.* BET bromodomain inhibition as a therapeutic strategy to target c-Myc. *Cell* 2011; **146**: 904–17.
16 Dervan PB, Doss RM, Marques MA. Programmable DNA binding oligomers for control of transcription. *Curr Med Chem Anticancer Agents* 2005; **5**: 373–87.
17 Dickinson LA, Burnett R, Melander C *et al.* Arresting cancer proliferation by small-molecule gene regulation. *Chem Biol* 2004; **11**: 1583–94.

18 Nickols NG, Szablowski JO, Hargrove AE *et al.* Activity of a py-im polyamide targeted to the estrogen response element. *Mol Cancer Ther* 2013; **12**: 675–84.
19 Yang F, Nickols NG, Li BC *et al.* Antitumor activity of a pyrrole-imidazole polyamide. *Proc Natl Acad Sci U S A* 2013; **110**: 1863–8.
20 Raskatov JA, Nickols NG, Hargrove AE *et al.* Gene expression changes in a tumor xenograft by a pyrrole-imidazole polyamide. *Proc Natl Acad Sci U S A* 2012; **109**: 16041–5.
21 Wang X, Nagase H, Watanabe T *et al.* Inhibition of MMP-9 transcription and suppression of tumor metastasis by pyrrole-imidazole polyamide. *Cancer Sci* 2010; **101**: 759–66.
22 Nickols NG, Jacobs CS, Farkas ME *et al.* Modulating hypoxia-inducible transcription by disrupting the HIF-1-DNA interface. *ACS Chem Biol* 2007; **2**: 561–71.
23 Matsuda H, Fukuda N, Ueno T *et al.* Transcriptional inhibition of progressive renal disease by gene silencing pyrrole-imidazole polyamide targeting of the transforming growth factor-beta1 promoter. *Kidney Int* 2011; **79**: 46–56.
24 Kang JS, Meier JL, Dervan PB. Design of sequence-specific DNA binding molecules for DNA methyltransferase inhibition. *J Am Chem Soc* 2014; **136**: 3687–94.
25 Taniguchi M, Fujiwara K, Nakai Y *et al.* Inhibition of malignant phenotypes of human osteosarcoma cells by a gene silencer, a pyrrole-imidazole polyamide, which targets an E-box motif. *FEBS Open Bio* 2014; **4**: 328–34.
26 Chen M, Matsuda H, Wang L *et al.* Pretranscriptional regulation of Tgf-beta1 by PI polyamide prevents scarring and accelerates wound healing of the cornea after exposure to alkali. *Mol Ther* 2010; **18**: 519–27.
27 Fernandez PC, Frank SR, Wang L *et al.* Genomic targets of the human c-Myc protein. *Genes Dev* 2003; **17**: 1115–29.
28 Hermeking H, Rago C, Schuhmacher M *et al.* Identification of CDK4 as a target of c-MYC. *Proc Natl Acad Sci U S A* 2000; **97**: 2229–34.
29 Chou CJ, Farkas ME, Tsai SM *et al.* Small molecules targeting histone H4 as potential therapeutics for chronic myelogenous leukemia. *Mol Cancer Ther* 2008; **7**: 769–78.
30 Chou CJ, O'Hare T, Lefebvre S *et al.* Growth arrest of BCR-ABL positive cells with a sequence-specific polyamide-chlorambucil conjugate. *PLoS One* 2008; **3**: e3593.
31 Berg T, Cohen SB, Desharnais J *et al.* Small-molecule antagonists of Myc /Max dimerization inhibit Myc-induced transformation of chicken embryo fibroblasts. *Proc Natl Acad Sci U S A* 2002; **99**: 3830–5.
32 Yao EH, Fukuda N, Ueno T *et al.* A pyrrole-imidazole polyamide targeting transforming growth factor-beta1 inhibits restenosis and preserves endothelialization in the injured artery. *Cardiovasc Res* 2009; **81**: 797–804.
33 Farkas ME, Li BC, Dose C *et al.* DNA sequence selectivity of hairpin polyamide turn units. *Bioorg Med Chem Lett* 2009; **19**: 3919–23.

34 Arvanitakis L. Yaseen N. Sharma S. Latent membrane protein-1 induces cyclin D2 expression, pRb hyperphosphorylation, and loss of TGF-beta 1-mediated growth inhibition in EBV-positive B cells. *J Immunol* 1995; **155**: 1047–56.

35 Wang YD. Dziegielewski J. Wurtz NR *et al.* DNA crosslinking and biological activity of a hairpin polyamide-chlorambucil conjugate. *Nucleic Acids Res* 2003; **31**: 1208–15.

36 Mateyak MK. Obaya AJ. Sedivy JM. c-Myc regulates cyclin D-Cdk4 and -Cdk6 activity but affects cell cycle progression at multiple independent points. *Mol Cell Biol* 1999; **19**: 4672–83.

37 Nickols NG. Dervan PB. Suppression of androgen receptor-mediated gene expression by a sequence-specific DNA-binding polyamide. *Proc Natl Acad Sci U S A* 2007; **104**: 10418–23.

38 Synold TW. Xi B. Wu J *et al.* Single-dose pharmacokinetic and toxicity analysis of pyrrole-imidazole polyamides in mice. *Cancer Chemother Pharmacol* 2012; **70**: 617–25.

39 Li S. Perlman DM. Peterson MS *et al.* Translation initiation factor 4E blocks endoplasmic reticulum-mediated apoptosis. *J Biol Chem* 2004; **279**: 21312–7.

40 Tu L. Liu Z. He X *et al.* Over-expression of eukaryotic translation initiation factor 4 gamma 1 correlates with tumor progression and poor prognosis in nasopharyngeal carcinoma. *Mol Cancer* 2010; **9**: 78.

41 Lin CJ. Nasr Z. Premsrirut PK *et al.* Targeting synthetic lethal interactions between Myc and the eIF4F complex impedes tumorigenesis. *Cell Rep* 2012; **1**: 325–33.

Supporting Information

Additional supporting information may be found in the online version of this article:

Doc. S1. Supplementary materials and methods.

Doc. S2. Reference list.

Fig. S1. Antiproliferative effect of Myc-5.

Fig. S2. Myc-5 localizes into nucleus.

Fig. S3. *In vivo* binding of Myc-5 at CDK4 gene promoter.

Fig. S4. Heat map represents the functional annotated transcripts that are identified by unpaired two-class significance analysis of microarray analysis with a false discovery rate of 0% from cells treated with DMSO (control), mismatch polyamide, and Myc-5.

Table S1. FITC-labeled oligomer sequences designed for EMSA

Table S2. Primers used in quantitative RT-PCR

Table S3. Primers used for ChIP real-time PCR

Table S4. Promoter-associated E-box genes

Table S5. Kinetic constant for Myc-5 pyrrole–imidazole polyamide and mismatch binding